Structure-guided design of a pure orthosteric antagonist of integrin αIIbβ3 that inhibits thrombosis but not clot retraction

Brian D. Adair [1,2,3], José L. Alonso [1,2,3], Johannes van Agthoven [1,2,3], Vincent Hayes [4], Hyun Sook Ahn [4], Jian-Ping Xiong[1,2,3], Mortimer Poncz [4], M. Amin Arnaout [1,2,3*]

[1] Leukocyte Biology & Inflammation Program, Massachusetts General Hospital, Boston, Massachusetts 02114, USA. [2] Division of Nephrology, Department of Medicine, Massachusetts General Hospital, Boston, Massachusetts 02114, USA. [3] Harvard Medical School, Boston, MA 02115, USA. [4] Division of Hematology, The Childrens Hospital of Philadelphia, Philadelphia, PA 19104

[*] Correspondence should be addressed to M.A.A. (email: aarnaout1@ mgh.harvard.edu).

Platelet integrin αIIbβ3 plays a critical role in both hemostasis and thrombosis. Current αIIbβ3 antagonists are potent anti-thrombotic drugs, but also cause adverse outcomes, which limited their clinical use. Drug-induced serious bleeding, thrombocytopenia and paradoxical thrombosis have been linked to impaired clot retraction and to conformational changes in αIIbβ3 that promote binding of preformed antibodies, natural ligands or both to αIIbβ3. We have used structure-guided design to generate the orthosteric inhibitor Hr10 that acts as a pure αIIbβ3 antagonist, i.e. it does not induce the conformational changes in αIIbβ3. Hr10 is as effective as the partial agonist drug eptifibatide in blocking platelet aggregation and arteriolar thrombosis in mice. In contrast to eptifibatide, however, Hr10 preserved thrombin-induced clot retraction, suggesting that it may not perturb hemostasis. Our structure-based approach can find general utility in designing pure orthosteric inhibitors for other integrins, in providing vital tools for dissecting structure-activity relationships in αIIbβ3, and potentially in offering safer alternatives for human therapy.

Platelet activation and accumulation at the site of blood vessel injury are the initial steps in hemostasis. Activated platelets adhere to the disrupted surface and aggregate upon binding of αIIbβ3 to soluble fibrinogen [1,2]. Fibrin generated by thrombin at or near the platelet surface also binds αIIbβ3, driving clot retraction [3], thereby consolidating the integrity of the hemostatic plug, restoring blood flow and promoting wound closure [4]. Excessive platelet activation after rupture of atherosclerotic plaques, for example, may lead to formation of occlusive thrombi, which are responsible for acute myocardial infarction and stroke, leading causes of death in developed countries [5]. It may also contribute to fibril formation in cerebral vessels of Alzheimer's disease patients [6]. The three parenteral αIIbβ3 antagonists (eptifibatide, tirofiban and abciximab) have demonstrated efficacy in reducing death and ischemic complications in victims of heart attacks [7]. However, their clinical use in acute coronary syndrome has been associated with significant risk of bleeding. And orally active anti-αIIbβ3 agents administered to patients at risk of acute coronary syndromes and other cardiovascular diseases were abandoned because of unexpected increased risk of patient death, linked to paradoxical thrombosis [8-10]. These adverse outcomes have limited use of direct αIIbβ3 antagonists to high-risk cardiac patients undergoing primary percutaneous coronary interventions [11,12], and contributed to the development of alternative anti-platelet drugs such as inhibitors of the adenosine diphosphate (ADP) receptor P_2Y_{12} and the thrombin receptor PAR1, both activators of αIIbβ3, but use of these drugs still causes serious bleeding [13,14].

Biochemical and clinical studies showed that the three anti-αIIbβ3 drugs are partial agonists, triggering conformational changes in αIIbβ3 that paradoxically enhance its binding to physiologic ligand thus promoting thrombosis [15,16], and also expose neo-epitopes in αIIbβ3 for natural antibodies, causing immune thrombocytopenia [17]. These drugs further increase bleeding risk by impairing clot retraction [18-20], which may require cessation of therapy, putting heart attack victims at high risk of re-thrombosis. Concluding that αIIbβ3 antagonism and partial agonism are inseparable, pharmaceutical companies veered away from further drug development directly targeting αIIbβ3.

The X-ray structures of unoccupied and ligand-bound αVβ3 ectodomain [21,22] elucidated the structural basis of ligand binding and the associated conformational changes in the integrin. These studies showed that ligand binding triggers tertiary changes in the ligand-binding βA domain of the β3 subunit, comprising the inward movement of the α1 helix (reported by β3-Tyr^{122}) towards the metal ion at the *m*etal *i*on-*d*ependent *a*dhesion *s*ite (MIDAS) and reshaping the F-α7 loop and the α7 helix. These changes trigger quaternary shape shifts including a swing-out movement of the hybrid domain underneath βA [23], leading to integrin genu-extension from its default genu-bent conformation (reviewed in [24]). These shape shifts expose neoepitopes in integrin αIIbβ3 for both natural antibodies and conformation-sensitive mouse monoclonal antibodies (mAbs), and promote physiologic ligand binding in the absence of an activating agent [16,25]. More recently, we showed that the global shape-shifts in αVβ3 are prevented by binding of the first "pure" αVβ3 antagonist, hFN10, a mutant form of the 10th type III domain of fibronectin (FN10)[26]. This is achieved by formation of a π-π interaction between the β3-Tyr^{122} of the inactive integrin with the indole derivative, tryptophan, that immediately follows the RGD motif of hFN10 [26]. However, the general applicability of this approach for generating pure antagonists for other integrins has not been explored.

In this report, we use the crystal structure of αVβ3/hFN10 complex (4mmz.pdb) to generate the peptide Hr10. Hr10 binds αIIbβ3 and maintains pure orthosteric integrin inhibition. Hr10 effectively blocks platelet aggregation induced not only by ADP but also by collagen or thrombin receptor activating peptide (TRAP). Hr10 is as effective as the partial agonist eptifibatide (Integrlin®) in inhibiting thrombosis in a mouse model that is used as predictor of clinical efficacy of platelet agents [27]. Unexpectedly, and in contrast to eptifibatide, Hr10 did not block clot retraction at effective anti-thrombotic concentrations. These data show the feasibility of using our structure-based approach to develop pure antagonists of other integrins, and suggest that such agents could offer safer and effective therapeutic alternatives to current anti-integrin drugs.

Results

Development of Hr10. The inability of hFN10 to bind αIIbβ3 [28] was investigated by superimposing the crystal structure of eptifibatide-bound αIIbβ3 (2vdn.pdb) onto that of hFN10-bound αVβ3 [26] (Figure 1). This analysis revealed a potential clash involving residues Ser^{1500}-Lys of the C-terminal F-G loop of hFN10 and Val^{156}-Glu in the longer helix-containing D2-A3 loop of the αIIb propeller domain. In addition, the shorter ligand Arg^{1493} of hFN10 cannot make the critical bidentate salt bridge with αIIb-Asp^{224} in the deeper pocket of the αIIb propeller (Figure 1). We therefore substituted Ser^{1500}-Lys in hFN10 with Gly, and replaced the ligand Arg^{1493} with the longer L-homoarginine (Har) as described [29], changes that we predicted would not adversely affect FN10 folding or the apparently key π-π interaction between β3-Tyr^{122} and Trp^{1496}, and would make Hr10 a novel ligand for αIIbβ3. The site-specific replacement of Arg^{1493} with Har^{1493} in the resulting ligand-mimetic peptide Hr10 was confirmed by mass spectroscopy (Supplementary Fig. 1).

Hr10 binds and blocks soluble fibrinogen binding to αIIbβ3. We first assessed if the introduced sequence changes affected binding of Hr10 to cellular β3 integrins. This was

determined by quantifying binding of Hr10 and hFN10 to the erythroleukemic cell line K562 stably expressing recombinant αIIbβ3 (αIIbβ3-K562) or αVβ3 (αVβ3-K562) in buffer containing 1mM each of Ca^{2+} and Mg^{2+}. Hr10 but not hFN10 bound αIIbβ3-K562 (Fig.2a) but maintained its capacity to bind αVβ3-K562 vs. hFN10, which only bound αVβ3-K562 (Fig.2a). We next compared the effects of Hr10, hFN10 and eptifibatide on soluble fibrinogen (FB) binding to αIIbβ3 preactivated by binding of mAb PT-25-2 [30], (αIIbβ3 preactivation is required for binding of physiologic ligand). Hr10 inhibited binding of Alexa647-labeled FB to preactivated αIIbβ3 in a dose dependent manner (Figure 2b), and was ~2-fold more effective in this function when compared to eptifibatide (IC_{50} for Hr10 calculated from the curves fit to the points yielded 30.3±4.8 nM [mean ± S.E., n=3] vs. 73.2 ± 7.0 nM for eptifibatide ($p=1.79x10^{-5}$)). hFN10 bound minimally to activated αIIbβ3-K562, with an order of magnitude greater IC_{50} of 474.0±73.4 nM (Figure 2b).

Crystal structure of αVβ3/Hr10 complex. To elucidate the structural basis of Hr10 binding to both β3 integrins, we soaked Hr10 into preformed αVβ3 ectodomain crystals (crystal packing of the αIIbβ3 ectodomain does not allow access of large peptides to the integrin binding site). A diffraction dataset to 3.1 Å was obtained for the αVβ3/Hr10 complex (Table 1). Clear densities for Hr10 and the metal ions at LIMBS, MIDAS and ADMIDAS were seen at the RGD-binding pocket (Figure 2c). The ligand Har^{1496} (replacing Arg) is lined with αV-Tyr^{178} and αV-Asp^{218}, and forms a bidentate salt bridge with αV-Asp^{218}, and a cation-π interaction with αV-Tyr^{178}, but does not contact αV-Thr^{212} (which replaces αIIb-Asp^{224}). The ligand Asp^{1495} directly coordinates the metal ion at MIDAS. Significantly, Trp^{1496} of Hr10 is able to make a π-π interaction with βA-Tyr^{122}, stabilized by an S-π interaction with βA-Met^{180} (Figure 2c) and by a hydrogen bond between the carbonyl of Trp^{1496} and Nε of βA-Arg^{214}, contacts also seen in the αVβ3/hFN10 structure [26]. Binding of Hr10 freezes the βA domain in the inactive conformation by preventing the activating inward movement of the α1 helix (reported by β3-Tyr^{122}) towards MIDAS, and the large change in the F-α7 loop [26]. Superposition of the βA domains from the αVβ3/Hr10 and αIIbβ3/eptifibatide structures show that the introduced Ser^{1500}-Lys/Gly substitution removes the predicted clash with the helical residues in the D2-A3 loop of the αIIb propeller (Figure 2d, compare with Figure 1). Nε, Nh1 and Nh2 amino groups of the ligand Har^{1493} superpose well on those of Har^{2} in eptifibatide, and could likewise form the bidentate salt bridge with αIIb-Asp^{224} as in the αIIbβ3/eptifibatide structure, accounting for the ability of Hr10 to also bind αIIbβ3 and block its binding to soluble FB.

Binding of Hr10 does not induce the activating conformational changes in αIIbβ3 and prevents ADP-induced αIIbβ3 activation. Binding of eptifibatide to human platelets at the clinically-effective plasma concentration of 1.5 μM in the absence or presence of 5 μM ADP induced global conformational changes in αIIbβ3, as reported by binding of the activation-sensitive and extension-sensitive mAbs AP5 [31] and LIBS-1 [32], respectively (Figure 3a, b). In contrast, Hr10 at 1.5 μM did not induce binding of AP5 or LIBS-1 to platelet αIIbβ3 and also suppressed AP5 and LIBS-1 binding to ADP-preactivated platelets (Figure 3a, b). These data suggest that Hr10 can reverse the global conformational changes in platelet αIIbβ3 triggered by ADP.

Effects of Hr10 on platelet aggregation and secretion. Next, we compared the effects of Hr10 and eptifibatide on human platelet aggregation in whole blood using standard concentrations of three agonists: collagen (1μg/ml), ADP (20 μM), and TRAP (10 μM). Hr10 was as effective as eptifibatide in blocking collagen-induced platelet aggregation, but was slightly (~2-fold) less effective in blocking aggregation induced by ADP or TRAP (Figure 4a-d).

Agonist-induced platelet activation is accompanied by release of the contents of α-granules, dense (δ-) granules and lysosomes, through fusion of these organelles with the plasma membrane. Both Hr10 and eptifibatide at the saturating 1.5 μM concentration (which inhibited platelet aggregation completely) blocked early ATP secretion from dense granules in whole blood following platelet activation with 20 μM ADP (Figure 4e). Hr10 inhibited ATP secretion by 71 ± 14 %, which is comparable to that seen with eptifibatide (60 ± 20 %)(Figure 4e). Secretion from human platelet α-granules (reported by CD62 expression) and lysosomal degranulation (reported by CD63 expression) in presence of Hr10 or eptifibatide were comparable following activation with 20 μM ADP (Figure 4f). Due to platelet aggregation, it was not possible to measure the amount of α-granule secretion and lysosomal degranulation following ADP activation in the absence of inhibitors. Abciximab and tirofiban are also reported to exert no [33,34] or only partial [35] inhibition of platelet α-granule secretion

Hr10 does not inhibit thrombin-induced clot retraction. Thrombin-induced clot retraction has been shown to positively correlate with the increased bleeding risk associated with use of eptifibatide and tirofiban [18-20]. We quantified the effect of Hr10 vs. eptifibatide, each at the saturating anti-aggregatory concentration of 1.5 μM, on thrombin-induced clot retraction in fresh human platelet-rich plasma (PRP) [36]. The kinetics of clot retraction were determined from quantification of serial images of the reaction acquired every 15 minutes for the 2-hour duration of the assay. As shown in Figure 5a-g, the kinetics of clot retraction in the absence or presence of Hr10 were nearly identical. In contrast, eptifibatide significantly inhibited clot retraction, as previously shown [20,37]. It has been proposed that anti-αIIbβ3 drugs that block both platelet aggregation and clot retraction bind inactive and active αIIbβ3 with similar high affinity [3]. As shown in Figure 5h, however, dose-response curves showed that affinity of Hr10 to inactive αIIbβ3 (IC_{50} =58.8±24.1 nM, 9 determinations of 5 experiments) is not significantly different from that to PT-25-activated αIIbβ3 (IC_{50} 35.2±5.7 nM, n=3 experiments; p=0.054), and is comparable to the affinity of eptifibatide to resting platelets (k_D=120 nM) [38].

Hr10 blocks microvascular thrombosis in vivo. To evaluate the effects of Hr10 vs. eptifibatide on nascent thrombus formation under flow, we used the thrombin-mediated arteriolar injury model in mice, known to predict the clinical efficacy of anti-platelet agents [27]. We used NSG (NOD-*scid-IL-2Rγ*^{null}) mice [39] that were also homozygous for human von Willebrand factor R1326H ($VWF^{RH/RH}$), which switches preferential binding from mouse to human glycoprotein (GP) Ib/IX, thus promoting incorporation of human over mice platelets into thrombi [40]. Use of these humanized mice is necessary as Hr10, like eptifibatide [27], binds poorly to mouse αIIbβ3 (not shown). Hr10 and eptifibatide in

equimolar concentrations were equally effective in preventing nascent occlusive thrombus formation at sites of laser-induced arteriolar injury (Figure 6).

Discussion

Hr10 is the first high affinity RGD-based inhibitor to function as a pure antagonist of αIIbβ3. A previous study showed that a non-RGD small molecule, RUC-2, also binds αIIbβ3 without activating this receptor; it works by occupying the Arg pocket in αIIb and destabilizing the Mg^{2+} at MIDAS, effects reversed, however, at high Mg^{2+} concentrations [41]. Hr10 makes multiple contacts with the ligand-binding βA domain, accounting for its stable high affinity binding to the integrin. The ability to generate a pure antagonist for another integrin, guided by the crystal structure of the αVβ3/hFN10 complex [26], suggests that existing RGD-like partial agonists like eptifibatide or tirofiban could be similarly engineered into new pure orthosteric antagonists.

Hr10 shared with eptifibatide the ability to effectively block soluble FB binding to activated αIIbβ3 as well as agonist-induced platelet aggregation at nearly equivalent IC_{50}s (varying only by two fold in either direction). At the clinically effective eptifibatide concentration of 1.5 μM, Hr10 was as effective in blocking ATP secretion *in vitro* and arteriolar thrombosis *in vivo*. One major difference from eptifibatide, however, is the ability of Hr10 to prevent the activating shape-shifts in the integrin that initiate proadhesive outside-in signaling [42]. This was evidenced by inhibition of binding of the activation-sensitive mAb AP5 and the extension-sensitive mAb LIBS-1 to αIIbβ3. Hr10 not only fails to initiate conformational changes on its own but also prevented the conformational changes in αIIbβ3 induced by inside-out signaling generated through binding of ADP to the P_2Y_{12} platelet receptor. The crystal structure of Hr10 in complex with αVβ3 revealed the structural basis of this pure antagonism: Hr10 froze βA in the inactive conformation, enabled by the central π-π contact of Hr10-Trp^{1496} with β3-Tyr^{122}. The dual specificity of Hr10 to both β3 integrins is also explained by the ability of Hr10's homoarginine to make a salt bridge with αV-Asp^{218}, and expectedly with αIIb-Asp^{224}. β3-Tyr^{122} is replaced with Phe^{122} in mouse β3, and the stabilizing salt bridge β3-Arg^{214} makes with β3-Asp^{179} is replaced with a H-bond with β3-Asn^{179} in mouse, both substitutions likely contributing to the poor binding of Hr10 to mouse αIIbβ3.

Hr10 is also distinguished from eptifibatide by its ability to preserve thrombin-induced clot retraction at equimolar concentrations that fully inhibit agonist-induced platelet aggregation. Clot retraction occurs in response to αIIbβ3-fibrin mediated actomyosin interaction [4,19], and is thought to secure hemostasis *in vivo*, as evidenced by increased bleeding in mice with impaired clot retraction [43], as well as in recipients of all three current clot-retraction inhibitory anti-αIIbβ3 drugs [18,20,37]. The underlying mechanism(s) for this unexpected difference between Hr10 and eptifibatide is not entirely clear. It has recently been shown that polymeric fibrin binds αIIbβ3 with higher affinity when compared with monomeric FB [44], suggesting that the high affinity of the three current anti-αIIbβ3 drugs is necessary to block fibrin-αIIbβ3 interaction and hence clot retraction. However, Hr10 and eptifibatide have nearly equivalent IC_{50}s in blocking soluble FB binding to activated αIIbβ3 and in inhibiting agonist-induced platelet aggregation. Others have found that drug candidates that block both platelet aggregation and clot retraction

bind with similar high affinity to active and inactive αIIbβ3, whereas those that block only aggregation have an affinity that is 2-3 logs lower to inactive vs. active αIIbβ3 [3,45]. Our data, however, shows no significant differences in high affinity binding of Hr10 to inactive and active αIIbβ3 (Fig. 5h). A recent study showed that fibrin binds αIIbβ3 even when its RGD-motifs (C-terminal γA chain motif essential for FB binding, and the two αA chain RGD motifs) are deleted [44], indicating the presence of additional fibrin binding sites in αIIbβ3 that mediate fibrin-dependent clot contraction. These were recently localized in the αIIb propeller domain, i.e. are distinct from MIDAS [46]. Previous studies have also shown that non-activated platelets can adhere to surface-immobilized fibrin(ogen) [47,48]. Thus one interpretation of the present data is that occupancy of non-RGD binding sites in Hr10-bound αIIbβ3 by polymeric insoluble fibrin still allows the αIIbβ3-dependent intracellular tyrosine de-phosphorylation required for clot retraction, a process otherwise blocked by eptifibatide-bound αIIbβ3 [37]. The availability of pure orthosteric antagonists of αIIbβ3 should provide a vital tool to dissect the contribution of integrin conformation to platelet function.

The dual specificity of Hr10 to both β3 integrins is shared with the drug abciximab [49]. Hr10, likewise, may be able to simultaneously prevent αVβ3-mediated thrombin generation, smooth muscle cell migration and proliferation, properties thought to contribute to the long-term clinical benefits of abciximab in acute coronary syndromes [50] [51]. In addition, dual specificity to both β3 integrins has previously shown a wide range of anticancer effects (reviewed in [52]). Dual β3 antagonism with abciximab, for example, was effective at blocking tumor growth and angiogenesis through targeting the interaction of tumor cells with platelets and endothelial cells, in addition to direct effects on the tumor tissue [53-56]. Hr10, a minor variant of a natural ligand that also does not prevent clot retraction, offers an attractive clinical candidate over abciximab, whose use has been associated with both immunogenicity and serious bleeding.

A commonly held view in the field is that effective inhibition of thrombosis by targeting αIIbβ3 cannot be achieved without compromising hemostasis, thus causing significant bleeding and increased morbidity and mortality. The data presented in this communication show that the pure ligand-mimetic antagonist Hr10, at concentrations that completely inhibit agonist-induced platelet aggregation *in vitro* and thrombosis *in vivo*, not only blocks integrin shape-shifting that can trigger immune thrombocytopenia or paradoxical thrombosis, but also preserves thrombin-induced clot retraction. These findings suggest that pure orthosteric inhibition of αIIbβ3 may offer a safer antithrombotic strategy with minimal perturbation of hemostasis.

Methods

Reagents and antibodies. Restriction and modification enzymes were obtained from New England Biolabs Inc. (Beverly, MA). Cell culture reagents were purchased from Invitrogen Corp (San Diego, CA) or Fisher Scientific (Hampton, NH). Mouse mAbs AP5 and LIBS-1 were kindly provided, respectively, by T.J. Kunicki (Blood Centre, Madison, WI) [31] and Dr. M. Ginsberg (University of California, San Diego) [32]. The Fab fragment of AP5 was prepared by papain digestion followed by anion exchange and size-exclusion chromatography. mAb PT-25-2 was the kind gift of Dr. Makoto Handa (Keio University, Tokyo, Japan) [30]. Hybridoma producing the β3 conformation-insensitive mAb AP3 was bought from ATCC and the antibody purified by Protein-A affinity chromatography. Alexa Fluor 488-conjugated mAbs directed against human CD62 and CD63 were bought from Santa Cruz Biotechnology, Dallas, TX. Alexa Fluor647-conjugated anti human CD42b mAb was purchased from R&D Systems, Minneapolis, MN. APC-labeled goat anti-mouse Fc-specific antibody was from Jackson ImmunoResearch (West Grove, PA). Alexa Fluor 647-conjugated Penta-His mAb was purchased from Qiagen, Germantown, MD. The plasmid pCDF5-Har, containing two copies of a UAG recognizing tRNA and the tRNA synthase (Har-Rs) for charging UAG tRNAs with Har, and the *E. coli* strain B-95ΔA containing a deletion of release factor 1 (*prfA)* and 95 synonymous TAG stop codon mutations, were kindly provided Dr. Kensaku Sakamoto (RIKEN, Yokohama, Japan) [29]. L-Har and TRAP-6 were purchased from Bachem. ADP, collagen, ATP, Chrono-luminescence reagent and human thrombin were purchased from Chrono-log (Havertown, PA).

Plasmids, mutagenesis, protein expression, purification and mass spectrometry. Human αVβ3 ectodomain was expressed in insect cells and purified as described [26]. hFN10 was expressed in BL21-DE3 bacteria and purified by affinity chromatography on nickel columns followed by gel filtration as described [26]. hFN10 containing a TAG stop codon at position 1493 was generated by PCR-based mutagenesis with the Quick-change kit (Agilent Technologies), cloned into bacterial expression plasmid pET11a and verified by DNA sequencing. Hr10 was expressed in B-95ΔA containing plasmids pCDF5-Har and pET-11a/hFN10-TAG in LB media supplemented with 5 mM L-Har, 50 μg/ml kanamycin (pCDF5-Har) and 100 μg/ml ampicillin (pET-11a). Cultures at ~0.5 A (600 nm) were induced with 0.3 mM IPTG and grown for 8 hours at room temperature. Hr10 was purified as for hFN10. Mass Spectrometry of purified Hr10 was performed at the Taplin Biological Mass Spectrometry Core Facility at Harvard Medical School (Boston MA) as described in [57].

Cell lines, cell culture and transfection. Human αVβ3-K562 cells have been previously described [26]. K562 cells stably expressing αIIβ3 (αIIβ3-K562) were kindly provided by Jennifer Cochran (Stanford University, CA) [58]. K562 cells were maintained in Iscove's modified Dulbecco's medium plus G418 (0.5–1.0 mg/ml), supplemented with 10% fetal calf serum, 2mM L-glutamine, penicillin and streptomycin.

Ligand binding and flow cytometry. For ligand binding assays, αIIβ3-K562 or αVβ3-K562 cells (1×10^6) were suspended in 100μl of WB (20 mM Hepes, 150 mM NaCl, pH 7.4, containing 0.1% [w/v] bovine serum albumin and 1mM each of $MgCl_2$ and $CalCl_2$)

and incubated first with Hr10 or hFN10 (each at 3-10 μg/ml) for 30 min at room temperature (RT). After washing, cells were incubated for 30 additional minutes at 4°C with Alexa Fluor 647 conjugated Penta-His mAb. Integrin expression was independently analyzed for each condition by incubating cells with the Alexa647-conjugated AP3 (10 μg/ml) for 30 min on ice. Cells were washed, re-suspended, fixed in 2% paraformaldehyde and analyzed using FACSCalibur or BD-LSRII flow cytometers (BD Biosciences). Ligand binding was expressed as mean fluorescence intensity (MFI), as determined using FlowJo software. Mean and SD from independent experiments were calculated, and compared using Student's t test.

For ligand binding competition studies, 100μl of PT-25-activated αIIbβ3-K562 (1×10^6) were incubated for 30 minutes at RT with serially diluted concentrations of Hr10, hFN10 or eptifibatide in the presence of 0.5 μM Alexa647-conjugated FB. Cells were washed, fixed in 2% paraformaldehyde and analyzed by flow cytometry. Ligand binding was expressed as IC_{50} of cells in the absence of competitor ligands. Mean and SD from three independent experiments were calculated, and compared using Student's t test.

Platelet aggregation and ATP secretion. Platelet aggregation and ATP secretion in whole blood were performed in a Chrono-Log model 700 two-channel lumi-aggregation system following the manufacturer's instructions. Blood was drawn from healthy volunteers directly into 3.2% sodium citrate and used within 3 hours. For impedance aggregation measurements, 0.5 ml of blood was mixed with 0.5 ml physiologic saline supplemented with inhibitors and incubated at 37° C for 5 minutes without stirring. Measurements were performed with stirring at 1,200 rpm at 37° C. Values for each data point represent impedance measurements following application of agonist integrated over 5 minutes. Data points for an individual dose curve were serially collected from a single draw and analyzed with SigmaPlot (Systat Software, San Jose, CA) using a least-square fit to a logistic curve and the IC_{50} value determined from the fitted parameter. ATP secretion proceeded similarly except that 0.45 ml of whole blood were added to 0.45 ml of saline supplemented with various concentrations of Hr10 or eptifibatide to produce the desired concentration at 1.0 ml. Following incubation for 5 minutes at 37° C, 100 μl of Chrono-lume reagent was added and aggregation initiated. The luminescence signal was quantified with a non-aggregated sample supplemented with an ATP standard.

Binding of mAbs. αVβ3-K562 cells or transiently transfected HEK293T (0.5×10^6 in 100 μl WB) were incubated in the absence or presence of unlabeled Hr10 or eptifibatide, each at 1.5μM, for 20 min at RT. Alexa647-labeled AP5 Fab or unlabeled anti-LIBS-1 (each to 10 μg/ml) were added, and cells incubated for an additional 30 min before washing. Alexa647-labeled AP3 was used for normalization of integrin expression. APC-labeled goat anti-mouse Fc-specific antibody was added to anti-LIBS-1-bound cells for an additional 30 min at 4°C, cells washed and processed for flow cytometry. Binding of anti-CD62 and anti-CD63 mAbs to platelets was performed by incubating (20 min, RT) 100 μl of ligand-pretreated 3.2% sodium citrate whole blood with either Alexa488-labeled mAb (at 10 μg/ml) in the presence of 10 μg/ml Alexa647-labeled anti-CD42b. Cells were fixed in 2% paraformaldehyde and CD62 and CD63 expression was analyzed by flow cytometry in the CD42b positive population.

Crystallography, structure determination and refinement. Human αVβ3 ectodomain was purified and crystallized by the hanging drop method as previously described [21]. Hr10 was soaked for 3 weeks into the preformed αVβ3 crystals at 1.5 mM in the crystallization well solution containing 1 mM Mn^{2+}. Crystals were harvested in 12% PEG 3500 (polyethylene glycol, molecular weight 3500), in 100 mM sodium acetate, pH 4.5, 800 mM NaCl plus 2 mM Mn^{2+} and FN10 (at 1.5 mM), cryoprotected by addition of glycerol in 2% increments up to 24% final concentration, and then flash-frozen in liquid nitrogen. Diffraction data was collected at ID-19 of APS, indexed, integrated, scaled by HKL2000 [59], and solved by molecular replacement using 3IJE as the search model in PHASER [60]. The structure was refined with Phenix [61] using translation-liberation-screw, automatic optimization of X-ray and stereochemistry, and Ramachandran restriction in the final cycle. Data collection and refinement statistics are shown in Table 1. The coordinates and structure factors of αVβ3/Hr10 have been deposited in the Protein Data Bank under accession code 6NAJ. Structural illustrations were prepared with Chimera [62].

Cremaster laser injury animal studies. Human blood was collected in 0.129 M sodium citrate (10:1 vol/vol). Platelet-rich plasma (PRP) was separated after centrifugation (200*g*, 10 minutes) at room temperature (RT). The platelets were then isolated from PRP, and prostaglandin E1 (Sigma-Aldrich) added to a final concentration of 1 μM. Platelets were then pelleted by centrifugation (800*g*, 10 minutes) at RT. The pellet was washed in calcium-free Tyrode's buffer (134 mM NaCl, 3 mM KCl, 0.3 mM NaH_2PO_4, 2 mM $MgCl_2$, 5 mM HEPES, 5 mM glucose, 0.1% $NaHCO_3$, and 1 mM EGTA, pH 6.5), and re-suspended in CATCH buffer (PBS and 1.5% bovine serum albumin, 1 mM adenosine, 2 mM theophylline, 0.38% sodium citrate, all from Sigma-Aldrich). Platelet counts were determined using a HemaVet counter (Drew Scientific). Intravital microscopy was performed as previously described [63 64]. $vWF^{RH/RH}$NSG male mice were studied after being anesthetized using sodium pentobarbital (80 mg/kg) injected intraperitoneally. Mice were maintained under anesthesia with the same anesthetic delivered via a catheterized jugular vein at 5 mg/ml throughout the experiment. The cremaster muscle was surgically exteriorized and continuously superfused with a physiological buffer (PBS containing 0.9 mM $CaCl_2$ and 0.49 mM $MgCl_2$) maintained at 37°C throughout the entire experiment and equilibrated with a mixture of 95% N2 and 5% CO2. Human platelets, 400 million per mouse, were labeled with mouse anti-human CD41 F(ab′)2 (BD Biosciences) conjugated to Alexa Fluor-488 and infused into the jugular vein, followed by Alexa Fluor-647 rat anti-mouse CD41 F(ab′)2 (Thermo Fisher) to detect endogenous mouse platelets [65]. Vascular injury was induced with an SRS NL100 pulsed nitrogen dye laser (440 nm) focused on the vessel wall through the microscope objective. Each injury was followed for three minutes. Eptifibatide was used at 5μg/mouse (equivalent to the clinically effective dose of ~1.5 μM [66]) and Hr10 at the equimolar concentration (60 μg/mouse). Drugs were infused 5 minutes prior to injury via the jugular vein. Pre and post drug measurements were made in the same animal. Wide-field images of thrombi were recorded using a Hamamatsu ORCA Flash 4.0 V3 CMOS camera (Hamamatsu, Japan) coupled to a Excelitas X-Cite XLED light source. The microscope, cameras, and light sources were all controlled using Slidebook 6.0 software (Intelligent Imaging Innovations). Intensity of the fluorescent signal was used to measure incorporated platelets [64]. Eight injuries were made in each of four mice in each group.

Clot retraction assay. 750 µl of Tyrode's buffer supplemented with inhibitor was mixed in a glass culture tube with 200 µl of PRP and 5 µl red blood cells. Clotting was initiated by addition of 50 µl thrombin at 10 units/ml in saline and a sealed Pasteur pipette secured in the tube center. Digital photographs of the experiment were taken at 15-minute intervals over 2 hours. Images were analyzed with ImageJ software to determine the area occupied by the clot and plasma. Plots of the relative areas and linear regressions were performed with SigmaPlot (Systat Software, San Jose, CA).

Statistical calculations. Dose response experiments for whole blood aggregation and binding in K562 cells were conducted at least three times. Curve-fitting and statistical calculations were performed in SigmaPlot. The data points from each replicate were scaled to one another by an initial fit to a sigmoidal function to determine the minimum and maximum values. Data scaled to a maximum of 1 and a minimum of 0 were combined and fit to a sigmoidal curve to determine the IC_{50} value. The standard error for the IC_{50} estimate was calculated using the reduced χ^2 method. P-values comparing IC_{50}s from different inhibitors were determined using the global fit function in SigmaPlot. The two data sets were fit with all parameters separate and again where the IC_{50} value is shared between the data sets. Fisher's F statistic was calculated from the residual sum of squares and degrees of freedom for the unshared (SS_{un}, DF_{un}) and shared (SS_{sh}, Df_{sh}) with the equation $F=((SS_{sh}-SS_{un})/(DF_{sh}-DF_{un}))/(SS_{un}/DF_{un})$ and the P-value obtained from the F distribution. Linear regression fits to data from clot retraction experiments proceeded similarly. The Holm-Sidak test following one-way ANOVA (alpha=5.0%) was used to assess if the differences in human platelet accumulation in thrombi between Hr10 and eptifibatide-treated mice were significant. Each time point was analyzed individually, without assuming a consistent standard deviation.

Acknowledgements. We thank Mr. Ross Tomaino at Harvard Medical School for performing the Mass Spec analysis. This work was supported by NIH grants DK088327 and DK48549 (to MAA), DK101628 (to JVA) and R01HL142122 and P01HL040387 (to MP) from the National Institutes of Diabetes, Digestive and Kidney diseases (NIDDK) and Heart, Lung and Blood (NHLBI) of the National Institutes of Health.

Author contributions. MAA conceived and oversaw all experiments. BLD performed the aggregation and clot retraction assays. JLA designed and performed the ligand- and antibody binding studies. JVA, JXP and MAA performed the modeling and structural studies. VH, HSA and MP performed the *in vivo* animal studies. All authors interpreted data. MAA had the primary responsibility for writing the manuscript.

Competing financial interests. The authors declare no competing financial interests.

Data availability. The authors declare that all data supporting the findings of this study are available within the paper.

Table 1. Data collection and refinement statistics.

Data collection	**αVβ3/Hr10**
PDB Code	6NAJ
Beamline	ID19 at APS
Space group	$P3_221$
Unit cell dimensions (Å, ^{o})	a=b=129.7, c=308.2; α=β=90, γ=120
Resolution range (Å)	50-3.1
Wavelength (Å)	0.97932
Total reflections	1,044,981
Unique reflections	55,225 (5,444)*
Completeness	100 (100)
Redundancy	8.2 (8.0)
Molecules in asymmetric unit	1
Average I/σ	24.9 (2.0)
R_{merge} (%)	9.7 (100)
R_{meas} (%)	10.3 (100)
R_{sym} (%)	3.6 (38.8)
Wilson B-factor	59.6
Refinement statistics	
Resolution range (Å)	49.2-3.1
R_{factor} (%)	24.9 (33.9)
R_{free} (%)#	27.4 (38.9)
No. of atoms	13,498
Protein	13,137
Water	4
Mn^{2+}	8
Glc-NAc	349
Average B-factor for all atoms (Å^2)	71.1
r.m.s. deviations	
Bond lengths (Å)	0.004
Bond angles (°)	1.03
Ramachandran plot	
Most favored (%)	90.9
Allowed regions (%)	8.7
Outliers (%)	0.4
Clashscore (%)	7.7
Rotamer outliers (%)	2.4

* Values in parentheses are for the highest resolution shell (0.1Å)
# R_{free} was calculated with 5% of the data

References

1. Coller, B.S. & Shattil, S.J. The GPIIb/IIIa (integrin alphaIIbbeta3) odyssey: a technology-driven saga of a receptor with twists, turns, and even a bend. *Blood* **112**, 3011-3025 (2008).
2. Bennett, J.S. Platelet-fibrinogen interactions. *Ann N Y Acad Sci* **936**, 340-354 (2001).
3. Hantgan, R.R. & Mousa, S.A. Inhibition of platelet-mediated clot retraction by integrin antagonists. *Thromb Res* **89**, 271-279 (1998).
4. Tutwiler, V., Wang, H., Litvinov, R.I., Weisel, J.W. & Shenoy, V.B. Interplay of Platelet Contractility and Elasticity of Fibrin/Erythrocytes in Blood Clot Retraction. *Biophys J* **112**, 714-723 (2017).
5. Benjamin, E.J.*, et al.* Heart Disease and Stroke Statistics-2017 Update: A Report From the American Heart Association. *Circulation* **135**, e146-e603 (2017).
6. Donner, L.*, et al.* Platelets contribute to amyloid-beta aggregation in cerebral vessels through integrin alphaIIbbeta3-induced outside-in signaling and clusterin release. *Sci Signal* **9**, ra52 (2016).
7. Bosch, X., Marrugat, J. & Sanchis, J. Platelet glycoprotein IIb/IIIa blockers during percutaneous coronary intervention and as the initial medical treatment of non-ST segment elevation acute coronary syndromes. *Cochrane Database Syst Rev*, CD002130 (2013).
8. Cox, D., Brennan, M. & Moran, N. Integrins as therapeutic targets: lessons and opportunities. *Nat Rev Drug Discov* **9**, 804-820 (2010).
9. Ndrepepa, G.*, et al.* Correlates of poor outcome among patients with bleeding after coronary interventions. *Coron Artery Dis* **25**, 456-462 (2014).
10. Raab-Westphal, S., Marshall, J.F. & Goodman, S.L. Integrins as Therapeutic Targets: Successes and Cancers. *Cancers (Basel)* **9**(2017).
11. Ibanez, B.*, et al.* 2017 ESC Guidelines for the management of acute myocardial infarction in patients presenting with ST-segment elevation: The Task Force for the management of acute myocardial infarction in patients presenting with ST-segment elevation of the European Society of Cardiology (ESC). *Eur Heart J* **39**, 119-177 (2018).
12. Rubboli, A. & Patti, G. What is the Role for Glycoprotein IIb/IIIa Inhibitor Use in the Catheterization Laboratory in the Current Era? *Curr Vasc Pharmacol* **16**, 451-458 (2018).
13. Tsai, T.T.*, et al.* Increased risk of bleeding in patients on clopidogrel therapy after drug-eluting stents implantation: insights from the HMO Research Network-Stent Registry (HMORN-stent). *Circ Cardiovasc Interv* **3**, 230-235 (2010).
14. Tricoci, P.*, et al.* Thrombin-receptor antagonist vorapaxar in acute coronary syndromes. *N Engl J Med* **366**, 20-33 (2012).
15. Du, X.P.*, et al.* Ligands "activate" integrin alpha IIb beta 3 (platelet GPIIb-IIIa). *Cell* **65**, 409-416 (1991).
16. Hantgan, R.R. & Stahle, M.C. Integrin priming dynamics: mechanisms of integrin antagonist-promoted alphaIIbbeta3:PAC-1 molecular recognition. *Biochemistry* **48**, 8355-8365 (2009).
17. Bougie, D.W.*, et al.* Acute thrombocytopenia after treatment with tirofiban or eptifibatide is associated with antibodies specific for ligand-occupied GPIIb/IIIa. *Blood* **100**, 2071-2076 (2002).

18. Schwarz, M., *et al.* Conformation-specific blockade of the integrin GPIIb/IIIa: a novel antiplatelet strategy that selectively targets activated platelets. *Circ Res* **99**, 25-33 (2006).
19. Haling, J.R., Monkley, S.J., Critchley, D.R. & Petrich, B.G. Talin-dependent integrin activation is required for fibrin clot retraction by platelets. *Blood* **117**, 1719-1722 (2011).
20. Shen, B., *et al.* A directional switch of integrin signalling and a new anti-thrombotic strategy. *Nature* **503**, 131-135 (2013).
21. Xiong, J.P., *et al.* Crystal structure of the extracellular segment of integrin alpha Vbeta3. *Science* **294**, 339-345 (2001).
22. Xiong, J.P., *et al.* Crystal structure of the extracellular segment of integrin alpha Vbeta3 in complex with an Arg-Gly-Asp ligand. *Science* **296**, 151-155 (2002).
23. Xiao, T., Takagi, J., Coller, B.S., Wang, J.H. & Springer, T.A. Structural basis for allostery in integrins and binding to fibrinogen-mimetic therapeutics. *Nature* **432**, 59-67 (2004).
24. Arnaout, M.A., Goodman, S.L. & Xiong, J.P. Structure and mechanics of integrin-based cell adhesion. *Curr Opin Cell Biol* **19**, 495-507 (2007).
25. Hantgan, R.R., Stahle, M.C., Connor, J.H., Connor, R.F. & Mousa, S.A. AlphaIIbbeta3 priming and clustering by orally active and intravenous integrin antagonists. *J Thromb Haemost* **5**, 542-550 (2007).
26. Van Agthoven, J.F., *et al.* Structural basis for pure antagonism of integrin alphaVbeta3 by a high-affinity form of fibronectin. *Nat Struct Mol Biol* **21**, 383-388 (2014).
27. Magallon, J., *et al.* Humanized mouse model of thrombosis is predictive of the clinical efficacy of antiplatelet agents. *Circulation* **123**, 319-326 (2011).
28. Richards, J., *et al.* Engineered fibronectin type III domain with a RGDWXE sequence binds with enhanced affinity and specificity to human alphavbeta3 integrin. *J Mol Biol* **326**, 1475-1488 (2003).
29. Mukai, T., *et al.* Reassignment of a rare sense codon to a non-canonical amino acid in Escherichia coli. *Nucleic Acids Res* **43**, 8111-8122 (2015).
30. Tokuhira, M., *et al.* A novel regulatory epitope defined by a murine monoclonal antibody to the platelet GPIIb-IIIa complex (alpha IIb beta 3 integrin). *Thromb Haemost* **76**, 1038-1046 (1996).
31. Honda, S., *et al.* Topography of ligand-induced binding sites, including a novel cation-sensitive epitope (AP5) at the amino terminus, of the human integrin beta 3 subunit. *J Biol Chem* **270**, 11947-11954 (1995).
32. Frelinger, A.L., Du, X., Plow, E.F. & Ginsberg, M.H. Monoclonal antibodies to ligand-occupied conformers of integrin aIIbb3 (Glycoprotein IIb-IIIa) alter receptor affinity, specificty, and function. *J. Biol. Chem.* **266**, 17106-17111 (1991).
33. Massberg, S., Mueller, I., Besta, F., Thomas, P. & Gawaz, M. Effects of 2 different antiplatelet regimens with abciximab or tirofiban on platelet function in patients undergoing coronary stenting. *Am Heart J* **146**, E19 (2003).
34. Tsao, P.W., Forsythe, M.S. & Mousa, S.A. Dissociation between the anti-aggregatory & anti-secretory effects of platelet integrin alpha IIb beta 3 (GPIIb/IIIa) antagonists, c7E3 and DMP728. *Thromb Res* **88**, 137-146 (1997).
35. Klinkhardt, U., *et al.* Differential in vitro effects of the platelet glycoprotein IIb/IIIa

inhibitors abixicimab or SR121566A on platelet aggregation, fibrinogen binding and platelet secretory parameters. *Thromb Res* **97**, 201-207 (2000).
36. Tucker, K.L., Sage, T. & Gibbins, J.M. Clot retraction. *Methods Mol Biol* **788**, 101-107 (2012).
37. Osdoit, S. & Rosa, J.P. Fibrin clot retraction by human platelets correlates with alpha(IIb)beta(3) integrin-dependent protein tyrosine dephosphorylation. *J Biol Chem* **276**, 6703-6710 (2001).
38. Schror, K. & Weber, A.A. Comparative pharmacology of GP IIb/IIIa antagonists. *J Thromb Thrombolysis* **15**, 71-80 (2003).
39. Shultz, L.D.*, et al.* Human lymphoid and myeloid cell development in NOD/LtSz-scid IL2R gamma null mice engrafted with mobilized human hemopoietic stem cells. *J Immunol* **174**, 6477-6489 (2005).
40. Magallon, J., Egalka, M. & Diacovo, T.G. Humanizing thrombi in mice. *Trends Cardiovasc Med* **21**, 33-36 (2011).
41. Zhu, J.*, et al.* Structure-guided design of a high-affinity platelet integrin alphaIIbbeta3 receptor antagonist that disrupts Mg(2)(+) binding to the MIDAS. *Sci Transl Med* **4**, 125ra132 (2012).
42. Shattil, S.J., Kim, C. & Ginsberg, M.H. The final steps of integrin activation: the end game. *Nat Rev Mol Cell Biol* **11**, 288-300 (2010).
43. Leon, C.*, et al.* Megakaryocyte-restricted MYH9 inactivation dramatically affects hemostasis while preserving platelet aggregation and secretion. *Blood* **110**, 3183-3191 (2007).
44. Litvinov, R.I., Farrell, D.H., Weisel, J.W. & Bennett, J.S. The Platelet Integrin alphaIIbbeta3 Differentially Interacts with Fibrin Versus Fibrinogen. *J Biol Chem* **291**, 7858-7867 (2016).
45. Mousa, S.A., Khurana, S. & Forsythe, M.S. Comparative in vitro efficacy of different platelet glycoprotein IIb/IIIa antagonists on platelet-mediated clot strength induced by tissue factor with use of thromboelastography: differentiation among glycoprotein IIb/IIIa antagonists. *Arterioscler Thromb Vasc Biol* **20**, 1162-1167 (2000).
46. Podolnikova, N.P.*, et al.* The interaction of integrin alphaIIbbeta3 with fibrin occurs through multiple binding sites in the alphaIIb beta-propeller domain. *J Biol Chem* **289**, 2371-2383 (2014).
47. Savage, B. & Ruggeri, Z.M. Selective recognition of adhesive sites in surface-bound fibrinogen by glycoprotein IIb-IIIa on nonactivated platelets. *J Biol Chem* **266**, 11227-11233 (1991).
48. Hamaguchi, M., Bunce, L.A., Sporn, L.A. & Francis, C.W. Spreading of platelets on fibrin is mediated by the amino terminus of the beta chain including peptide beta 15-42. *Blood* **81**, 2348-2356 (1993).
49. Tam, S.H., Sassoli, P.M., Jordan, R.E. & Nakada, M.T. Abciximab (ReoPro, chimeric 7E3 Fab) demonstrates equivalent affinity and functional blockade of glycoprotein IIb/IIIa and alpha(v)beta3 integrins. *Circulation* **98**, 1085-1091 (1998).
50. Topol, E.J.*, et al.* Multi-year follow-up of abciximab therapy in three randomized, placebo-controlled trials of percutaneous coronary revascularization. *Am J Med* **113**, 1-6 (2002).
51. Admiral, I. Three-year duration of benefit from abciximab in patients receiving stents for acute myocardial infarction in the randomized double-blind ADMIRAL study.

Eur Heart J **26**, 2520-2523 (2005).
52. Sheldrake, H.M. & Patterson, L.H. Function and antagonism of beta3 integrins in the development of cancer therapy. *Curr Cancer Drug Targets* **9**, 519-540 (2009).
53. Trikha, M.*, et al.* Multiple roles for platelet GPIIb/IIIa and alphavbeta3 integrins in tumor growth, angiogenesis, and metastasis. *Cancer Res* **62**, 2824-2833 (2002).
54. Gomes, N.*, et al.* Breast adenocarcinoma cell adhesion to the vascular subendothelium in whole blood and under flow conditions: effects of alphavbeta3 and alphaIIbbeta3 antagonists. *Clin Exp Metastasis* **21**, 553-561 (2004).
55. Engebraaten, O., Trikha, M., Juell, S., Garman-Vik, S. & Fodstad, O. Inhibition of in vivo tumour growth by the blocking of host alpha(v)beta3 and alphaII(b)beta3 integrins. *Anticancer Res* **29**, 131-137 (2009).
56. Liu, Y.*, et al.* The roles of platelet GPIIb/IIIa and alphavbeta3 integrins during HeLa cells adhesion, migration, and invasion to monolayer endothelium under static and dynamic shear flow. *J Biomed Biotechnol* **2009**, 829243 (2009).
57. Zhang, S.*, et al.* Identification and characterization of a novel botulinum neurotoxin. *Nat Commun* **8**, 14130 (2017).
58. Silverman, A.P., Kariolis, M.S. & Cochran, J.R. Cystine-knot peptides engineered with specificities for alpha(IIb)beta(3) or alpha(IIb)beta(3) and alpha(v)beta(3) integrins are potent inhibitors of platelet aggregation. *J Mol Recognit* **24**, 127-135 (2011).
59. Otwinowski, Z. & Minor, W. *Processing of X-ray diffraction data collected in oscillation mode.*, (Academic Press, New York, 1997).
60. McCoy, A.J.*, et al.* Phaser crystallographic software. *J Appl Crystallogr* **40**, 658-674 (2007).
61. Adams, P.D.*, et al.* PHENIX: a comprehensive Python-based system for macromolecular structure solution. *Acta Crystallogr D Biol Crystallogr* **66**, 213-221 (2010).
62. Pettersen, E.F.*, et al.* UCSF Chimera--a visualization system for exploratory research and analysis. *J Comput Chem* **25**, 1605-1612 (2004).
63. Celi, A.*, et al.* Thrombus formation: direct real-time observation and digital analysis of thrombus assembly in a living mouse by confocal and widefield intravital microscopy. *J Thromb Haemost* **1**, 60-68 (2003).
64. Neyman, M., Gewirtz, J. & Poncz, M. Analysis of the spatial and temporal characteristics of platelet-delivered factor VIII-based clots. *Blood* **112**, 1101-1108 (2008).
65. Fuentes, R.E.*, et al.* A chimeric platelet-targeted urokinase prodrug selectively blocks new thrombus formation. *J Clin Invest* **126**, 483-494 (2016).
66. Holmes, M.B., Sobel, B.E. & Schneider, D.J. Variable responses to inhibition of fibrinogen binding induced by tirofiban and eptifibatide in blood from healthy subjects. *Am J Cardiol* **84**, 203-207 (1999).

FIGURE LEGENDS

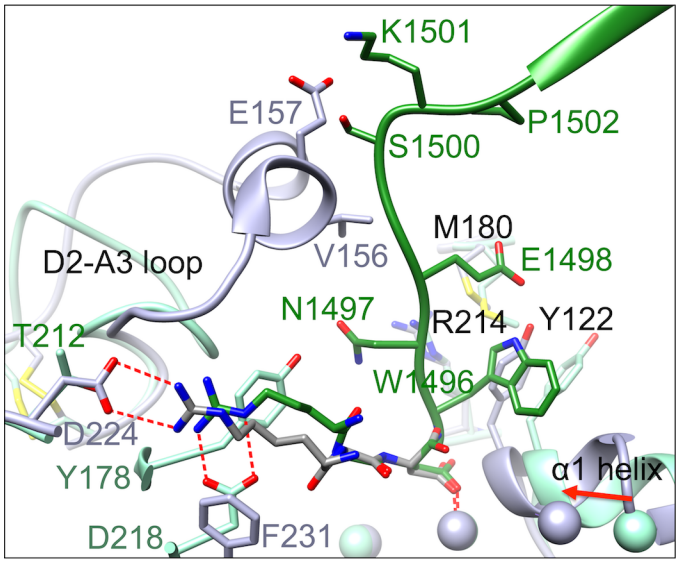

Figure 1. Structure-guided design of Hr10. Ribbon diagrams of crystal structures αVβ3/hFN10 (light green) and αIIbβ3/eptifibatide (light purple) superposed on the βA domain of each, with the metal ions at LIMBS, MIDAS and ADMIDAS shown as spheres in the respective colors. Relevant segments of the propeller and βA domains and of hFN10 (dark green) and eptifibatide (dark gray) are shown. The MIDAS ion is ligated by the aspartate residue from each ligand. Residues (single letter code) specific to each structure are shown in the respective color, with residues or loops common in both indicated in black. Oxygen, nitrogen, and sulfur atoms are in red, blue and yellow, respectively. The inward movement (red arrow) of the α1 helix and ADMIDAS ion in αIIbβ3, driven by binding of the partial agonist eptifibatide, is absent in hFN10-bound αVβ3, the result of a π-π interaction between ligand W^{1496} and β3-Y^{122}. β3-R^{214} and β3-M^{180} contribute to the stability of ligand W^{1496}. The homoarginine from eptifibatide forms a bidentate salt bridge with αIIb-D^{224} (replaced by T^{212} in αV), whereas R^{1493} of hFN10 contacts αV-D^{218} (replaced by F^{231} in αIIb). A clash between the c-terminal F-G loop of hFN10 and the longer D2-A3 loop of the αIIb propeller, replacement of D^{218} in αV with F^{231} in αIIb and the shorter side chain of R^{1493} (vs. homoarginine in eptifibatide) are predicted to account for the poor binding of hFN10 to αIIbβ3.

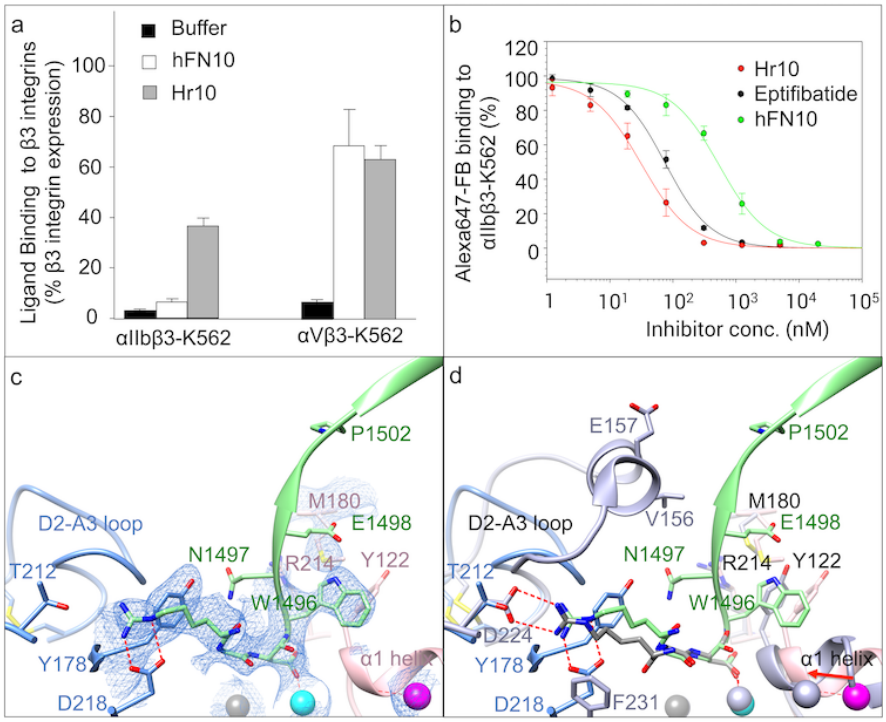

Figure 2. Binding properties and crystal structure of Hr10/integrin complex. a) FACS analysis of the binding of Hr10 and hFN10 (each at 1.5 μM) to αIIbβ3-K562 and αVβ3-K562 (mean±S.D., n=3 independent experiments). Bound ligand was detected with a labeled anti-His tagged mAb. Buffer represents binding of the anti-His antibody to cells without ligand. b) Dose response curves (mean±S.E., n=3 independent experiments) generated from FACS analysis showing displacement of Alexa-647 labeled fibrinogen bound to preactivated αIIbβ3-K562 by increasing concentrations of unlabeled Hr10, eptifibatide or hFN10. The MFI values from the FACS analyses were normalized individually before averaging as described in "methods". The IC_{50} values are stated in text. c) Ribbon diagram of the crystal structure of Hr10/αVβ3 complex showing the electron density map (blue mesh) at 1.0 σ of the ligand-binding region. Relevant portions of Hr10 (light green), αV propeller (light blue) and β3A domain (rose color) are shown. Side-chains are shown as sticks in the respective colors. Oxygen, nitrogen, and sulfur atoms are in red, blue and yellow, respectively. The Mn^{2+} ions at the LIMBS, MIDAS and ADMIDAS are in grey, cyan, and magenta spheres, respectively. Water molecules are not shown. The Hr10 ligand W^{1496} forms a π-π interaction with β3-Y^{122}, and Har^{1493} forms a bidentate salt bridge with αV-D^{218}. The view is identical to that in Fig. 1. d) Ribbon diagrams of the crystal structures of αVβ3/Hr10 (light green) and αIIbβ3/eptifibatide (light purple) superposed on the βA domain of each. The view is identical to that in (c) and in Fig.1. Nε, Nh1 and Nh2 amino groups of Har^{1493} superpose nicely onto those of Har^{2} of eptifibatide (dark gray). Domain, side chain and metal ion colors are as in Fig.1 and (c). Note the removal of the predicted clash of Hr10 with D2-A3 loop of αIIb and predicted formation of a bidentate salt bridge between ligand Har^{1493} and αIIb-D^{224}.

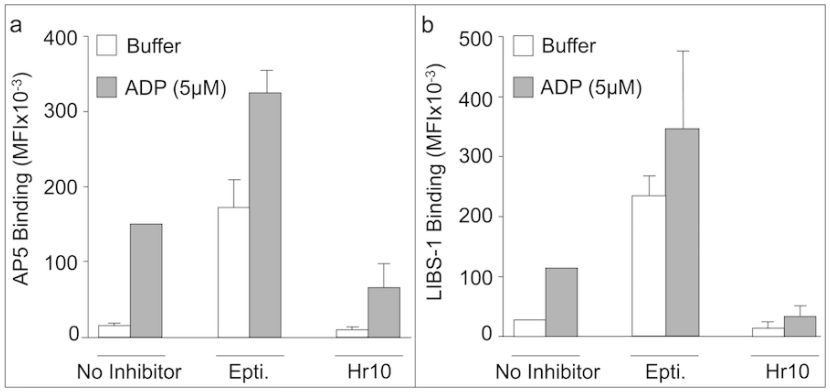

Figure 3. Hr10 suppresses the activating conformational changes in cellular αIIbβ3. a, b) Histograms (mean+S.D., n=3 independent experiments) showing effect of Hr10 vs. eptifibatide (1.5 μM each) on integrin shape shifting. Binding of the activation-sensitive mAb AP5 (a) or the extension-sensitive mAb LIBS-1 to human platelets in the absence or presence of ADP (5μM) was assessed following flow cytometry. Binding of the two conformation-sensitive mAbs to ADP-activated platelets in the absence of the inhibitors was often complicated by platelet aggregation, thus only single measurements could be obtained for each mAb.

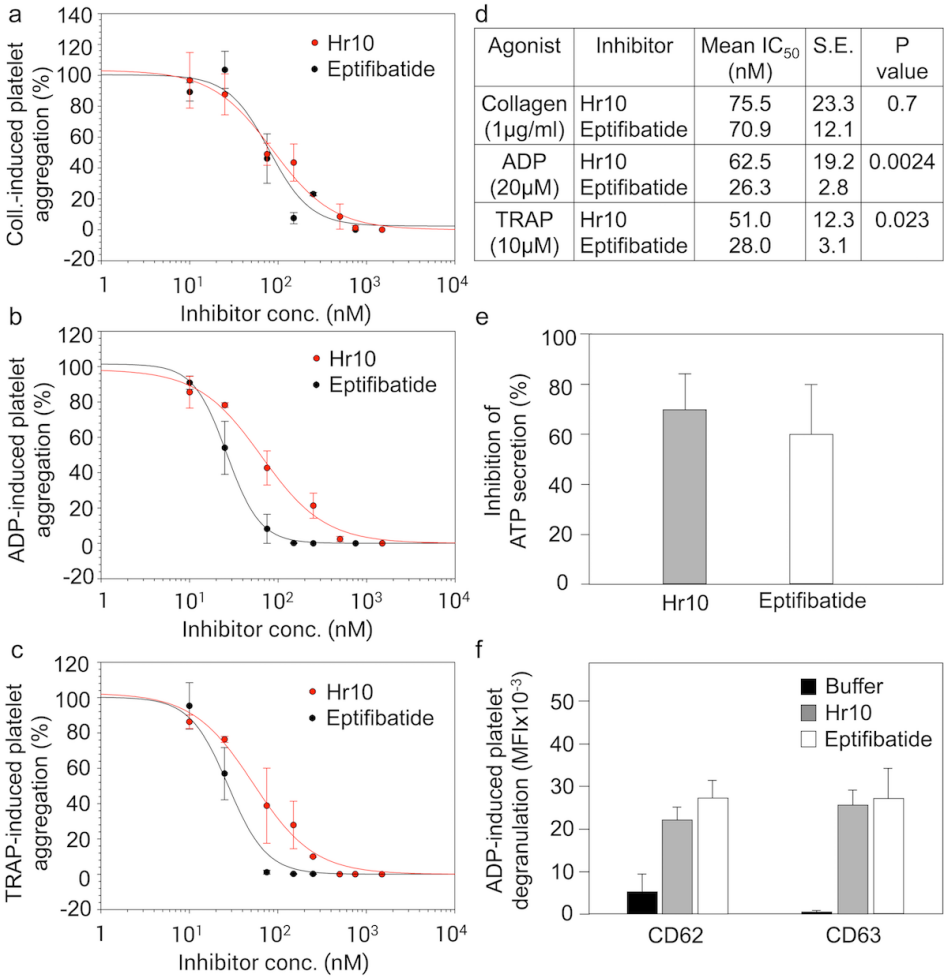

Agonist	Inhibitor	Mean IC_{50} (nM)	S.E.	P value
Collagen (1μg/ml)	Hr10 Eptifibatide	75.5 70.9	23.3 12.1	0.7
ADP (20μM)	Hr10 Eptifibatide	62.5 26.3	19.2 2.8	0.0024
TRAP (10μM)	Hr10 Eptifibatide	51.0 28.0	12.3 3.1	0.023

Figure 4. Effect of Hr10 and eptifibatide on platelet aggregation and secretion. (a-c) Dose response curves (mean ±S.E., n=3 experiments from 3 different donors) showing effects of the inhibitors on aggregation induced by collagen (2μg/ml) (a), ADP (20 μM) (b), or TRAP (10 μM) (c). Points for the integrated impedance from the three experiments were individually normalized prior to averaging and are displayed with least-squares fits to the mean values. The respective IC_{50}s, S.E. and p-values from an F-test are listed in (d). (e-f) Histograms (mean±S.D., n=3) showing the effect of the inhibitors (each at 1.5 μM) on ADP (20 μM)-induced ATP secretion (e), secretion of α-granules and lysosomal degranulation (f) from platelets followed with FACS analysis of labeled antibodies to the cell surface reporters CD62 and CD63, respectively.

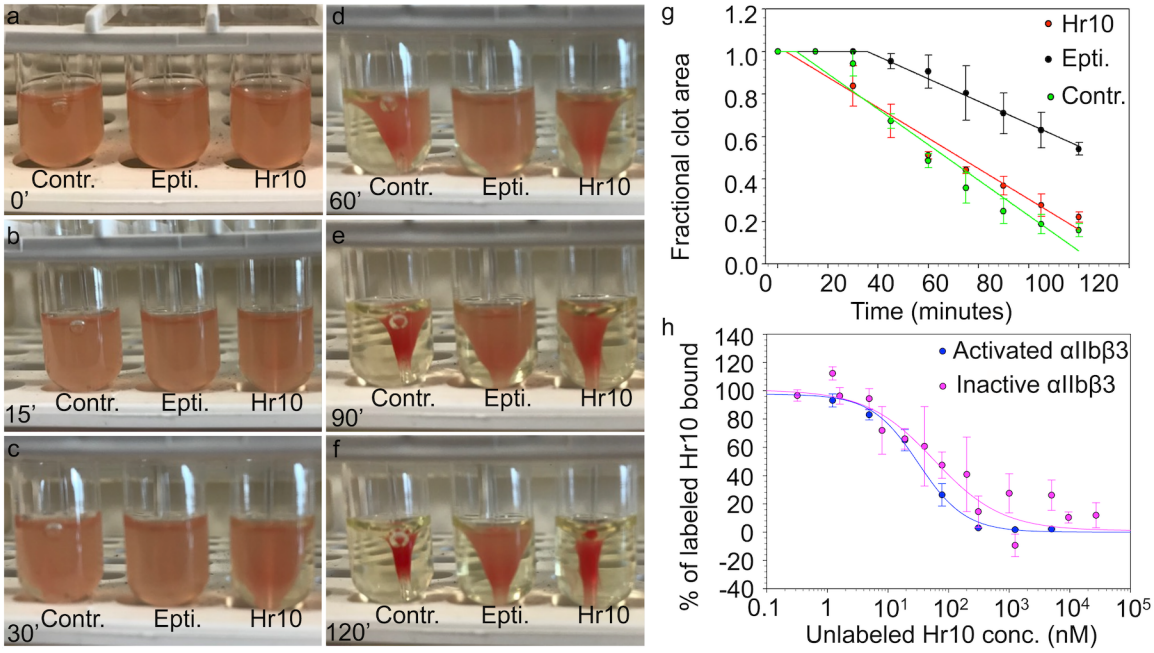

Figure 5. Effects of Hr10 and eptifibatide on thrombin-induced clot retraction. a-f) Kinetics of clot retraction in the absence (Contr.) or presence of Hr10 or eptifibatide (Epti.) from one representative experiment of three conducted. Clot retraction took place around a central glass rod. 5 µl of red blood cells were added per 1 ml reaction to enhance the color contrast for photography. Photographs shown were taken at 0 time and at 15, 30, 60, 90 and 120 minutes after addition of thrombin. (g) Time course (mean ±S.E.) from three clot retraction experiments including the one shown in a-f. The plot shows the fractional area occupied by the clot at 15-minute intervals with a linear regression through the points. A lag period of ~30 minutes is noted with eptifibatide. (h) Dose response curves comparing displacement of Alexa488-labeled Hr10 binding to PT-25-activated and to inactive αIIbβ3 on K562 cells by increasing concentrations of unlabeled Hr10. Cell binding was analyzed by FACS. The mean fluorescence intensity values for individual Hr10 experiments (three independent determinations for activated αIIbβ3, and five independent experiments, with two conducted in triplicates for inactive αIIbβ3) were initially fit with a binding curve to determine minimum and maximum MFI values to use in scaling the data. The points and error bars indicate the mean and standard error for the scaled data. The magenta and blue lines are a least squares fit to the averages.

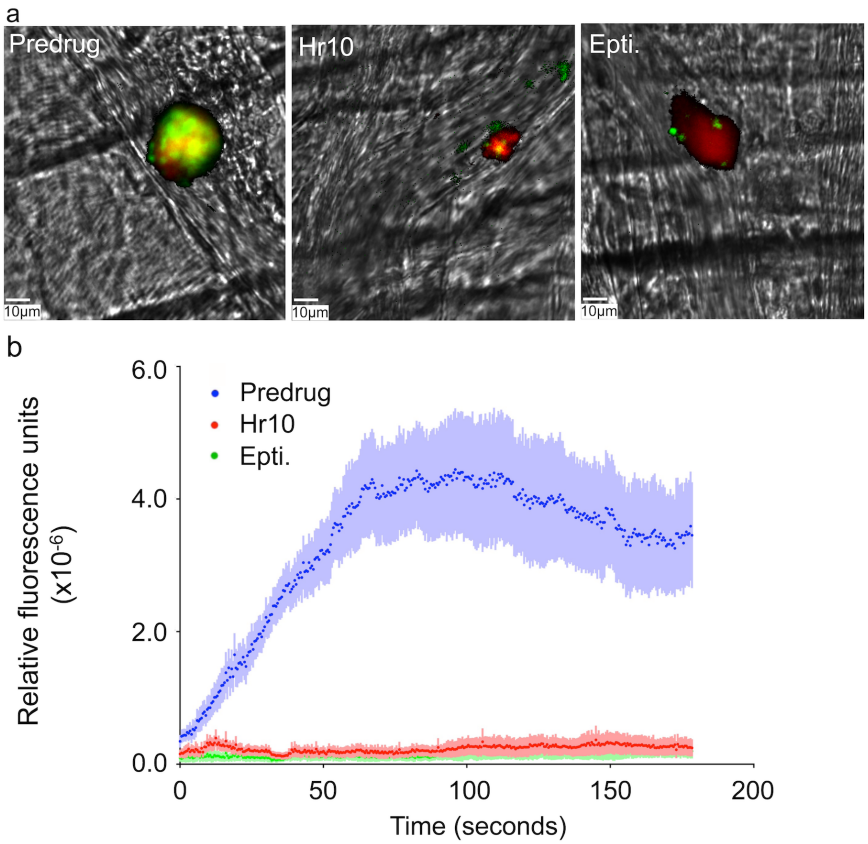

Figure 6. Hr10 inhibits laser-induced microvascular injury in mice. (a) Representative images of thrombi at 60s in absence (predrug) and presence of Hr10 or eptifibatide (Epti.). Micrographs are superimposed with fluorescent images for human platelets (green) and mouse platelets (red). (b) Graph showing kinetics (mean±S.E.) of human platelet accumulation at nascent injuries during infusion of PBS (predrug), or of equimolar amounts of Hr10 or eptifibatide (see text). *n*=4 animals per arm. There was no significant difference in human platelet accumulation in thrombi, between Hr10 and eptifibatide at each time point.